Modeling Inner Magnetospheric Electric Fields: Latest Self-Consistent Results

Stanislav Sazykin[1], Robert W. Spiro[1], Richard A. Wolf[1], Frank R. Toffoletto[1], Nikolai Tsyganenko[2], J. Goldstein[3], and Marc R. Hairston[4]

This paper presents some of the latest results of self-consistent numerical modeling of large-scale inner-magnetospheric electric fields obtained with the Rice Convection Model (RCM). The RCM treats plasma drifts, electric fields, and currents in the inner magnetosphere self-consistently in the quasi-static (slow-flow) approximation under the assumption of isotropic pitch-angle distribution. Event simulations of the magnetic storm of March 31, 2001 are used with two newly available RCM input models: an empirical model of the storm-time magnetospheric magnetic field, and an empirical model of the plasma sheet. Results show that the effect of severe distortion of the magnetic field during very large magnetic storms improves the ability of the RCM to predict the location of Sub-Auroral Polarization Stream (SAPS) events, although there is not perfect agreement with observations. Weakening of shielding by region-2 Birkeland currents during times of severe magnetic field inflation also improves comparison of the RCM-computed plasmapause location with data. Results of simulations with plasma boundary sources varying in response to measured solar wind inputs show that the plasma sheet may become interchange unstable under certain geomagnetic conditions.

1. INTRODUCTION

The large-scale physics of the inner magnetosphere can be investigated theoretically by solving time-dependent equations of particles drifting in an electric field self-consistently calculated from the current-continuity equation and a time-dependent assumed magnetic field [e.g., *Wolf*, 1983], an approach known as "convection modeling" [e.g., *Harel et al.*, 1981a,b].

The Rice Convection Model (RCM), a numerical code based on the quasi-static (slow-flow) approach [*Wolf*, 1983] and the theoretical tool of choice for this work, has been used extensively to explain or illuminate many observed large-scale dynamical phenomena in the inner magnetosphere (e.g., shielding by region-2 Birkeland currents of the low-latitude region from the main effects of magnetospheric convection, the formation and decay of the storm-time ring current, the shape of the plasmapause, generation of subauroral ion drift or polarization jet electric fields), and to study the possibility of interchange instability in the inner plasma sheet [e.g., *Toffoletto et al.*, 2003; *Sazykin et al.*, 2002].

Based on more than 30 years of extensive modeling and comparisons with observations, our understanding of the electrodynamics of this part of the magnetosphere is better than ever, though it is not without gaps. In this paper, we highlight several unresolved issues related to large-scale storm-time

[1] Physics and Astronomy Department, Rice University, Houston, Texas
[2] Universities Space Research Association and NASA Goddard Space Flight Center, Greenbelt, Maryland
[3] Space Science and Engineering Division, Southwest Research Institute, San Antonio, Texas
[4] Center for Space Sciences, University of Texas Dallas, Texas

The Inner Magnetosphere: Physics and Modeling
Geophysical Monograph Series 155

10.1029/155GM28

magnetospheric and ionospheric electric fields, and we present some of our latest results bearing on these issues. The results presented below are from RCM numerical simulations of the magnetic storm that took place on March 31, 2001.

Among the unresolved issues in the physics of the inner magnetosphere and magnetosphere-ionosphere coupling are the rapid westward flows that are observed equatorward of the diffuse aurora, typically in the dusk-midnight sector. Using instruments carried by early Russian spacecraft, *Galperin et al.* [1974] first discovered strong (>50 mV/m), narrow (~1° latitude) poleward ionospheric electric fields in this region and called them "polarization jets". They were independently reported in the U.S.A. [e.g., *Smiddy et al.*, 1977; *Maynard*, 1978; *Spiro et al.*, 1978] and termed SAID (Sub-Auroral Ion Drift) events by *Spiro et al.* [1979]. Recently, the term SAPS (Sub-Auroral Polarization Stream) was introduced to describe somewhat wider regions of less intense westward flow that occur in the same general region, primarily in major storms [*Foster and Burke*, 2002].

Southwood and Wolf [1978] proposed a mechanism for generation of enhanced subauroral electric fields that involves closure of dusk-side region-2 Birkeland currents across a region of low conductivity. Event simulations with the RCM [*Harel et al.*, 1981a,b] showed sub-auroral electric field structures consistent with *in-situ* electric field measurements and in agreement with the *Southwood and Wolf* [1978] explanation.

Despite this early (and subsequent) success in predicting observed SAPS, many event simulations have shown that the RCM has a tendency to predict SAPS that are weaker than those observed, with latitudinal locations that tend to be poleward of the observed SAPS. In this paper, we examine two of the three factors that we identify as being responsible for this discrepancy: the magnetic field model used with the RCM, and temporal variability in plasma sheet density and temperature during storms. The third relevant factor relates to details of the auroral contribution to the conductivity tensor at the equatorward edge of the diffuse aurora, which we will not address here. The same RCM simulations are also used to compare RCM-computed plasmapause shapes and locations with those derived from the Extreme Ultraviolet (EUV) imager on board the IMAGE spacecraft as an indication of how accurate the overall RCM-computed subauroral convection electric field is. Finally, initial results regarding electric field structures due to the interchange instability in the plasma sheet are presented and discussed.

2. MODEL AND EVENT DESCRIPTIONS

2.1. Rice Convection Model

As the RCM physics and numerical methods have been described by, among others, *Harel et al.* [1981a], *Wolf* [1983], *Sazykin et al.* [2002], and *Toffoletto et al.* [2003], our description here will be the minimum necessary for understanding of the results below.

In the slow-flow, closed-field-line region of Earth's magnetosphere, each chemical species s ($s = \{1,2,3\}$ for e^-, H^+, O^+) of charge q_s is assumed to be isotropic in pitch angle. At the model boundary, each species is assumed to have a $\kappa = 6$ distribution function. The distribution function is divided into K_s "channels" in terms of invariant energy λ, which is related to kinetic energy W through the flux-tube volume $V = \int ds/B$ as $\lambda_{k,s} = W_{k,s} \cdot V^{2/3}$ and remains invariant along drift trajectories. The particle content $\eta_{k,s}$ in channel s, expressed in terms of number density $n_{k,s}$ as $\eta_{k,s} = n_{k,s} \cdot V$, is another invariant except for source and loss terms. In the absense of plasma production, the evolution of $\eta_{k,s}$ is governed by an advection equation:

$$\left[\frac{\partial}{\partial t} + \frac{\mathbf{B} \times \nabla \left(\Phi + (\lambda_{k,s}/q_s) V^{-2/3}\right)}{B^2} \cdot \nabla\right] \eta_{k,s} = -L_{k,s} \quad (1)$$

where $L_{k,s}$ represents plasma loss mechanisms. The present runs include ion loss by charge-exchange and electron loss by precipitation. The electrostatic potential Φ satisfies the current conservation equation

$$\nabla \cdot \left(-\hat{\Sigma} \cdot \nabla \left(\Phi - \Phi_c\right)\right) = \frac{\mathbf{B}}{B} \cdot \nabla V \times \nabla P \quad (2)$$

where Φ_c transforms to a frame rotating with the Earth, and the field-aligned current on the right-hand side is expressed in terms of gradients of total particle pressure P and flux tube volume V. $\hat{\Sigma}$, the conductance tensor, includes contributions from both solar EUV (based on the IRI-90 empirical model) and from self-consistently estimated auroral electron precipitation at 30% of the strong pitch-angle scattering limit. There are no field-aligned potential drops.

The RCM solves $\Sigma_s K_s$ equations (1) and equation (2) iteratively, stepping in time. The main inputs to the model are the electric potential on the poleward boundary ("polar cap" potential) for (2) and the number density and temperature of particles at the poleward boundary for (1), which is assumed to be the only source of particles.

2.2. Magnetic Field Model

Equations (1) and (2) include the magnetic field, a quantity that is not calculated in the model but is instead a time-dependent input to it. Previously, for event studies we have used the theoretical magnetic field model of *Hilmer and Voigt* [1995] (HV). However, HV does not adequately represent inflation of the innermost magnetosphere during large disturbances, possibly contributing to the discrepancy

between the observed and RCM-predicted location and strength of subauroral electric field structures. Here, we present first results from using the new storm-time magnetic field model of *Tsyganenko et al.* [2003] (T03S); this magnetic field model is based on data from 37 large magnetic storms and was constructed to account for large distortions of the inner ($L < 10$) magnetosphere during storms.

2.3. Plasma Sheet Boundary Conditions

Since we neglect source terms such as ion outflow from the ionosphere in (2), the only source of particles into the modeling region (and therefore the storm-time ring current) is represented by the high-L boundary condition on η. Due to the scarcity of *in-situ* central plasma sheet data, the RCM has typically been used with constant boundary conditions. However, it is known that plasma sheet properties are directly correlated with solar wind properties. Therefore, for results presented here we have used the empirical plasma sheet model of *Tsyganenko and Mukai* [2003] to specify the number density and temperature of particle species at $(-13R_E,0,0)$ (GSM coordinates) as a function of solar wind density, velocity, and interplanetary magnetic field (IMF) B_z component. These values are assumed to be constant in local time along the boundary.

2.4. Magnetic Storm of March 31, 2001

A coronal mass ejection and related interplanetary shocks produced a large magnetic storm that started early on March 31, 2001. Figure 1 shows the solar wind dynamic pressure and the GSM z-component of the IMF measured by SWEPAM and MAG instruments on board the ACE spacecraft (time-shifted to the sub-solar magnetopause location), together with the SYM-H index taken to represent Dst. Extreme solar wind conditions, including high dynamic pressure and large negative IMF B_z, occurred intermittently and produced extreme magnetospheric conditions, e.g., cross-polar cap potential drop in excess of 200 kV, strong ring current, dayside magnetopause earthward of geosynchronous orbit, and plasmapause locations inside 2 R_E at some local times.

During most of the day on March 30, the magnetic field below 66° latitude is quasi-dipolar. The degree of magnetic field distortion during the main phase of the storm can be seen in the equatorial mapping of lines of constant magnetic latitude and longitude. Figure 2 shows this mapping at ~08:30 UT, which is the time SYM-H reached its minimum value. The 56° magnetic latitude line that maps to $L = 3.2$ in a dipole field maps to 7 R_E at midnight in the disturbed field. The dominance of the tail current contribution to the *Dst* [*Skoug et al.*, 2003] is consistent with the field representation by T03S.

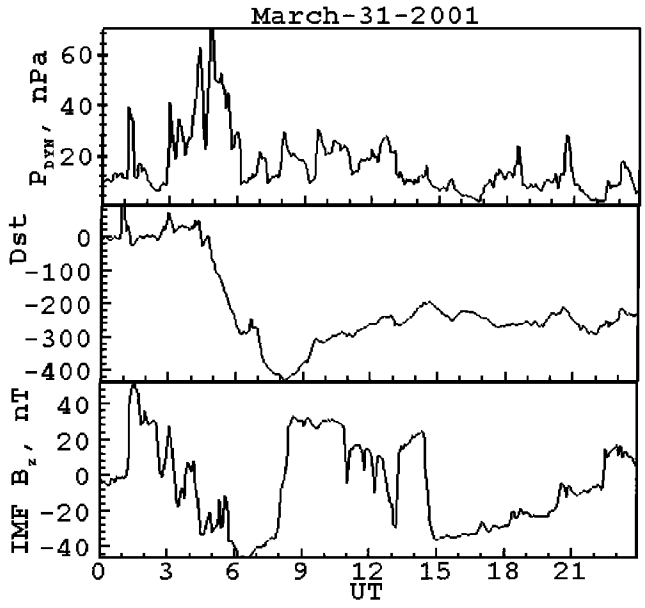

Figure 1. 5-min averaged solar wind dynamic pressure P_{dyn}, *Dst* (SYM-H) index, and the IMF B_z component for March 31, 2001. P_{dyn} and IMF B_z are from ACE time-shifted measurements.

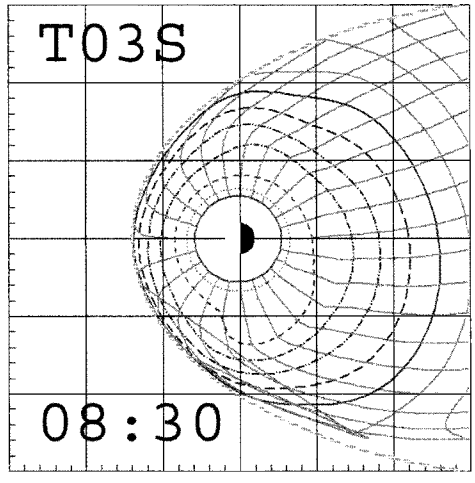

Figure 2. Mapping of lines of constant magnetic latitudes (innermost at 50°, step is 2°) and longitudes (step is 15°) to the equatorial plane using T03S magnetic field model, for ~08:30 UT on March 31, 2001 (time of Dst minimum).

The polar cap potential drop used as an input to the RCM was initially calculated from 5-minute averages of ACE solar wind and IMF data using the empirical relations of *Boyle et al.* [1997]. Since the polar cap potential apparently saturated at around 200 kV based on DMSP ion drift data [*Hairston et al.*, 2003], we have modified the expressions of

Boyle et al. so that if the potential drop exceeds 150 kV, the potential is reduced linearly to saturate at 200 kV.

Electric field measurements derived from DMSP drift meter and Millstone Hill incoherent-scatter radar data showed large subauroral electric field structures, which we identify as SAPS events. Simultaneous observations of total electron content (TEC) structures coincident with the plasmaspheric tails observed with the extreme ultraviolet (EUV) imager on board the IMAGE spacecraft, and subauroral electric field structures, have been reported by *Foster et al.* [2002].

3. RESULTS

We present results from three RCM simulations of this event. In the first two, we kept the plasma boundary condition constant throughout the event and varied the magnetic field model, using first the HV magnetic field model and then the T03S magnetic field model. Since T03S was found to improve our predicted electric fields (see below), a third simulation was done with T03S and with a time-varying plasma sheet boundary condition based on the empirical expressions of *Tsyganenko and Mukai* [2003].

3.1. Subauroral Electric Fields

Figure 3 compares the RCM-computed westward ion drift velocity (corresponding to poleward-directed electric field component perpendicular to **B**) in the ionospheric frame, obtained with HV and T03S magnetic fields. Superimposed is DMSP data along the spacecraft trajectory.

A SAPS, apparent as a secondary (equatorward) peak in the electric field, was seen by the DMSP ion drift meter and was also predicted by the RCM in both cases. While the location of the SAPS is in much better agreement with data in the T03S case, the magnitude of the peak is higher. A similar conclusion can be drawn from Figure 4, which is for roughly the same MLT in the subsequent pass, but in the southern hemisphere. A large uncertainty not addressed in these calculations (but the subject of ongoing research) is the dependence on details of the sub-auroral conductance distribution. Inaccuracies in our conductance model may well be responsible for the quantitative inaccuracy in our predictions of peak velocity in the SAPS.

3.2. Plasmapause

With launch of the IMAGE spacecraft and the subsequent availability of EUV He^+ 30.4 nm emission-based images of the plasmasphere, a new diagnostic tool has become available for indirect determination of the partially-shielded convection electric field in the innermost part of the magnetosphere. In the RCM, the location of the plasmapause is calculated by solving equation (2) for an electron energy "channel" with $\lambda = 0$ (cold) particles, which **E**×**B** drift in a time-dependent electric field. We compare this computed boundary shape with the plasmapause shape derived from EUV images based on gradients of the emission intensity as first reported by *Foster et al.* [2002] and subsequently verified by *Goldstein et al.* [2003].

Skoug et al. [2003] reported EUV plasmapause images for this storm. According to their analysis, the initial pre-storm

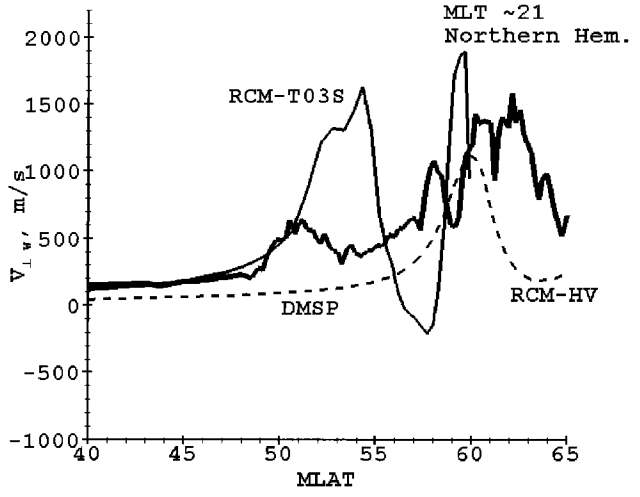

Figure 3. Westward ion drift (poleward electric field) component measured by the DMSP F15 ion drift meter along its trajectory for the pass that started at 15:06 UT, northern hemisphere (thick); RCM-computed ion drift component along the same trajectory (~21 MLT) obtained with T03S (solid thin) and HV (dashed) magnetic field.

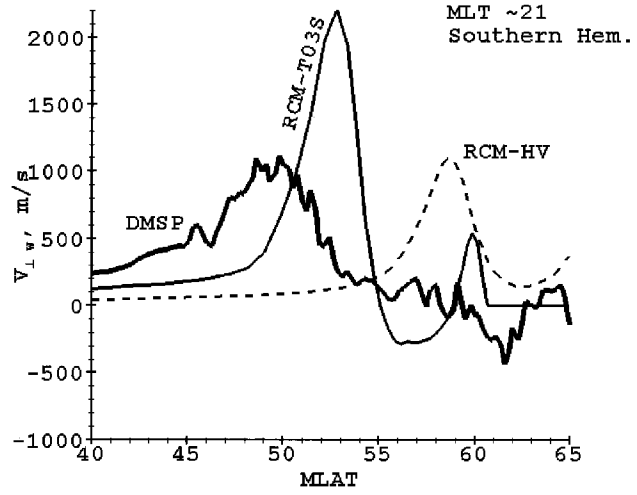

Figure 4. Same as Figure 3 but for the subsequent southern hemisphere pass.

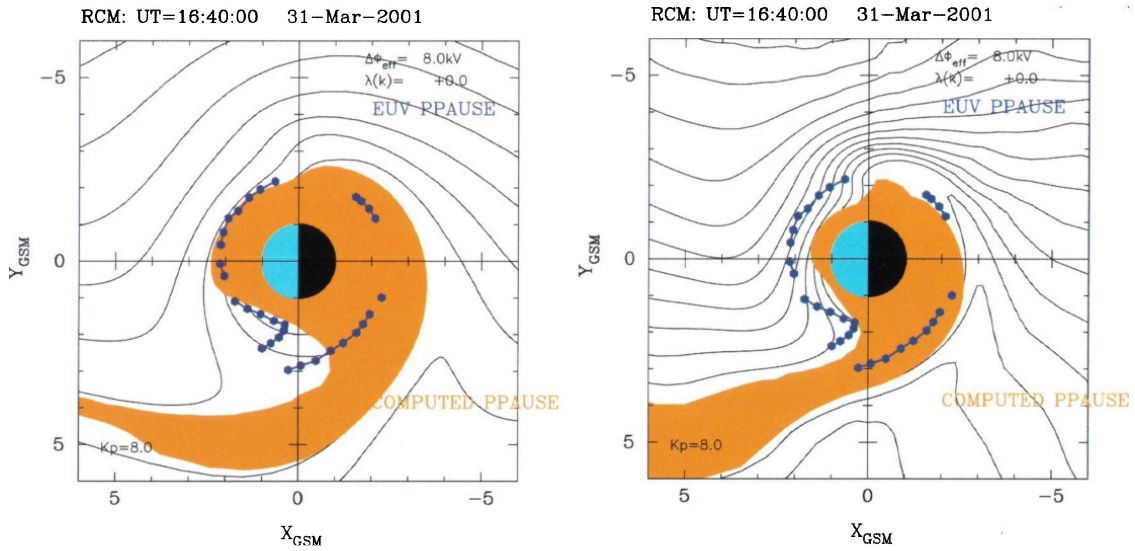

Plate 1. Comparison of the RCM-computed plasmapause boundary calculated with HV (left panel) and T03S (right panel), at 16:40 UT. The location of the boundary is shown by filling the entire plasmasphere with orange color. Contour lines are instantaneous flow lines for cold ($\lambda = 0$) particles. Superimposed on both plots is the location of the plasmapause derived from EUV image data (blue symbols).

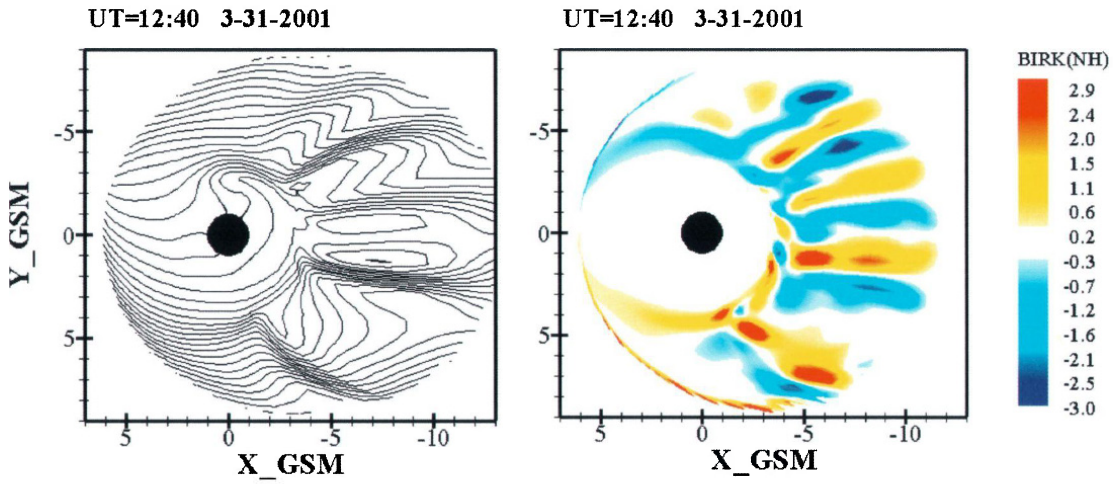

Plate 2. Structure of the ionospheric potential (left) and Birkeland currents (right) characteristic of the interchange instability, at 12:40 UT. Both quantities are mapped to the equatorial plane. Contour step for the potential is 5 kV. Currents are in $\mu A/m^2$.

shape of the plasmasphere was approximately circular, with the size of $L \sim 4$, and an indication of the a plasmaspheric tail at dusk. Our calculations at 00 UT on 3/31/2001 are in good agreement with the these observations. During the main phase of the storm, EUV images indicated a very strong plasmasphere contraction, to within $L \sim 2$ [*Skoug et al*, 2003]. Unfortunately, the quality of images during this period (03-07 UT) precluded derivation of the plasmapause location.

However, IMAGE-derived plasmapause locations were once again obtained for a period starting at ~15:30 UT. In Plate 1, we compare the IMAGE-derived shapes with those computed by the RCM using the HV and T03S magnetic field models. We should note that the algorithm for deriving EUV plasmapause locations is somewhat subjective, with the error estimated to be 0.1 to 0.4 R_E [*Goldstein et al.*, 2003]. Both RCM calculations and the data show a large plasmaspheric tail (plume) extending from the post-dusk plasmapause to the dayside magnetopause. While the dayside plasmapause location is more sensitive to the assumed distribution of the potential on the high-latitude boundary of the modeling region, the nightside plasmapause shape is mostly affected by the prompt-penetration electric field. In our experience, when compared to EUV data, the RCM tends to predict a larger plasmasphere on the nightside, especially near dusk. The discrepancy is larger for the HV case; with the T03S calculation giving better agreement with data.

The size of the plasmasphere is controlled by the strength of the convection and the effectiveness of region-2 Birkeland currents in shielding the subauroral latitudes from the convection electric field. Since for this storm, the plasmasphere was observed within $L \approx 2$, inflation of the magnetic field does not seem important. The shielding is weaker in the T03S case, allowing stronger electric fields on the nightside and thus making the plasmasphere smaller. Analysis of figures such as Plate 1 throughout the storm (not shown) leads us to conclude that the second discrepancy regarding larger bulge on the duskside is a persistent feature. Thus the RCM predictions for both the SAPS and the dusk-midnight plasmapause lie at higher L than the observations indicate.

3.3. Interchange Instability in the Plasma Sheet

Extreme variations of the solar wind and IMF parameters during this magnetic storm led us to investigate the susceptibility of the plasma sheet to the interchange instability. *Skoug et al.* [2003] reported geosynchronous *in-situ* particle observations of the plasma sheet being very close to the Earth and with number densities increasing more than a factor of 10 during the storm. The possibility of the inner edge of the plasma sheet and ring current becoming interchange-unstable has been demonstrated in an event simulation by *Sazykin et al.* [2002] (see also references therein). Solar wind control of the conditions for the interchange instability was discussed by *Golovchanskaya et al.* [2002].

When we allowed the RCM plasma sheet boundary conditions to vary in response to changing solar wind conditions, we found three intervals of interchange instability of the magnetosphere lasting from 30 min to 2 hours. An example of the resulting highly-structured electrostatic potential and field-aligned current patterns is shown in Plate 2. The primary physical effect of the interchange instability is to transport low-content flux tube "bubbles" earthward through the plasma sheet by forming elongated "fingers". An interesting consequence of this situation is its possible relevance to the formation of auroral arcs [*Golovchanskaya and Maltsev*, 2003].

4. SUMMARY

RCM simulations of the major magnetic storm of March 31, 2001 were used to compare RCM-computed electric fields with *in-situ* and remote sensing measurements.

The degree of inflation of the magnetic field controls the strength of the overall subauroral electric field, which can be seen in its influence on the shape and location of the plasmapause. Use of the T03S magnetic field model results in the RCM-computed nightside plasmapause being in a better agreement with IMAGE EUV data.

The inflation of the magnetic field also strongly affects the strength and the latitudinal location of the SAPS electric fields structures. Using T03S, which is arguably a better storm-time magnetic field model, results in the RCM predicting SAPS that are stronger and located more equatorward. This partially resolves the previous discrepancy between RCM-predicted and observed SAPS electric fields, although full agreement is still not achieved.

When the plasma sheet boundary condition is allowed to vary during the storm, model results indicate that the plasma sheet may become interchange unstable under certain solar wind conditions, although the details depend on several assumptions made in the calculations.

Acknowledgments. Work at Rice University was supported by the Upper Atmospheric Research division of the NSF under grant ATM-20101349 and by the NASA Sun-Earth Connection Theory Program under grant NAG5-11881. N.T. acknowledges support by grants from NASA's LWS (NAG5-12185) and NSF GEM (ATM-0296212) programs. The DMSP data were provided by support from NASA grant NAG5-9297. Work at Southwest Research Institute was supported by NASA SEC Guest Investigator grant NAG5-12787. We thank the ACE SWEPAM and MAG instrument teams and the ACE Science Center for providing the ACE data. SYM-H indices were obtained from Kyoto World Data Center for Geomagnetism, Japan.

REFERENCES

Boyle, C.B., P.H. Reiff, and M.R. Hairston, Empirical polar cap potentials, *J. Geophys. Res.*, 102, 111, 1997.

Foster, J.C., and W.J. Burke, ASPS: A new characterization for subauroral electric fields, *EOS*, 83, 393, 2002.

Foster, J.C., P.J. Erickson, A.J. Coster, J. Goldstein, and F.J. Rich, Ionospheric signatures of plasmaspheric tails, *Geophys. Res. Lett.*, 29, 1623, doi:10.1029/2002GL015067, 2002.

Galperin, Y.I., Y.N. Ponomarev, and A.G. Zosimova, Plasma convection in polar ionosphere, *Ann. Geophys.*, 30, 1-7, 1974.

Goldstein, J., M. Spasojevic, P.H. Reiff, B.R. Sandel, W.T. Forrester, D.L. Gallagher, and B.W. Reinisch, Identifying the plasmapause in IMAGE EUV data using IMAGE RPI in situ steep density gradients, *J. Geophys. Res.*, 108, 1147, doi:10.1029/2002JA009475, 2003.

Golovchanskaya, I.V., and Y.P. Maltsev, Interchange instability in the presence of the field-aligned current: Application to the auroral arc formation, *J. Geophys. Res.*, 108, 1106, doi:10.1029/2002JA009505, 2003.

Golovchanskaya, I.V., Y.P. Maltsev, and A.A. Ostapenko, High-latitude irregularities of the magnetospheric electric field and their relation to solar wind and geomagnetic conditions, *J. Geophys. Res.*, 107, 1001, doi:10.1029/2001JA900097, 2002.

Hairston, M.R., T.W. Hill, and R.A. Heelis, Observed saturation of the ionospheric potential during 31 March 2001 storm, *Geophys. Res. Lett.*, 30, 1325, doi:10.1029/2002GL015894, 2003.

Harel, M., R.A. Wolf, P.H. Reiff, R.W. Spiro, W.J. Burke, F.J. Rich, and M. Smiddy, Quantitative simulation of a magnetospheric substorm 1, Model logic and overview, *J. Geophys. Res.*, 86, 2217, 1981a.

Harel, M., R.A. Wolf, R.W. Spiro, P.H. Reiff, C.-K. Chen, W.J. Burke, F.J. Rich, and M. Smiddy, Quantitative simulation of a magnetospheric substorm 2, Comparison with observations, *J. Geophys. Res.*, 86, 2242, 1981b.

Hilmer, R.V., and G.-H. Voigt, A magnetospheric magnetic field model with flexible current systems driven by independent physical parameters, *J. Geophys. Res.*, 100, 5613-5628, 1995.

Maynard, N.C., On large poleward-directed electric fields at subauroral latitudes, *Geophys. Res. Lett.*, 5, 617, 1978.

Sazykin, S., R.A. Wolf, R.W. Spiro, T.I. Gombosi, D.L. De Zeeuw, and M.F. Thomsen, Interchange instability in the inner magnetosphere associated with geosynchronous particle flux decreases, *Geophys. Res. Lett.*, 29, 1448, doi:10.1029/2001GL014416, 2002.

Skoug, R.M., M.F. Thomsen, M.G. Henderson, H.O. Funsten, G.D. Reeves, C.J. Pollock, J.-M. Jahn, D.J. McComas, D.G. Mitchell, P.C. Brandt, B.R. Sandel, C.R. Clauer, and H.J. Singer, Tail-dominated storm main phase: 31 March 2001, *J. Geophys. Res.*, 108, 1259, doi:10.1029/2002JA009705, 2003.

Smiddy, M., M.C. Kelley, W. Burke, F. Rich, R. Sagalyn, B. shuman, R. Hays, and S. Lai, Intense poleward-directed electric fields near the ionospheric projection of the plasmapause., *Geophys. Res. Lett.*, 4, 543, 1977.

Southwood, D.J., and R.A. Wolf, An assessment of the role of precipitation in magnetospheric convection, *J. Geophys. Res.*, 83, 5227, 1978.

Spiro, R.W., R.A. Heelis, and W. B. Hanson, Ion convection and the formation of the mid latitude F-region ionospheric trough, *J. Geophys. Res.*, 84, 4255, 1978.

Spiro, R.W., R.A. Heelis, and W.B. Hanson, Rapid sub-auroral ion drifts observed by Atmospheric Explorer C, *Geophys. Res. Lett.*, 6, 657, 1979.

Toffoletto, F., S. Sazykin, R. Spiro, and R. Wolf, Inner magnetospheric modeling with the Rice Convection Model, *Space Science Rev.*, 107, 175-196, 2003.

Tsyganenko, N.A., and T. Mukai, Tail plasma sheet models derived from Geotail particle data, *J. Geophys. Res.*, 108, 1136, doi:10.1029/2002JA009707, 2003.

Tsyganenko, N.A., H.J. Singer, and J.C. Kasper, Storm-time distortion of the inner magnetosphere: How severe can it get? *J. Geophys. Res.*, 108, 1209, doi:10.1029/2002JA009808, 2003.

Wolf, R.A., The quasi-static (slow-flow) region of the magnetosphere, in *Solar-Terrestrial Physics,* edited by R.L. Carovillano and J.M. Forbes, 303, D. Reidel, Hingham, MA, 1983.

J. Goldstein, Space Science & Engineering Div., Southwest Research Institute, 6220 Culebra Rd., San Antonio, TX 78238.

M.R. Hairston, W.B. Hanson Center for Space Sciences, University of Texas Dallas, P.O. Box 830688 F022, Richardson, TX 75083.

S. Sazykin, R.W. Spiro, F.R. Toffoletto, R.A. Wolf, Physics and Astronomy Department, Rice University, MS-108, 6100 South Main St., Houston, TX 77005.

N.A. Tsyganenko, USRA/NASA Goddard Space Flight Center, Code 695, Greenbelt, MD 20771.